

Title: **Synthetic Seismograms at Regional Distances for May 1995 Earthquake and Explosion Sources in Western China**

Condensed Version

Author(s): Fred N. App, Randy J. Bos, James R. Kamm

Submitted to: **Project No. ST482A
Sponsored by U.S. Department of Energy**



Los Alamos
NATIONAL LABORATORY

Los Alamos National Laboratory, an affirmative action/equal opportunity employer, is operated by the University of California for the U.S. Department of Energy under contract W-7405-ENG-36. By acceptance of this article, the publisher recognizes that the U.S. Government retains a nonexclusive, royalty-free license to publish or reproduce the published form of this contribution, or to allow others to do so, for U.S. Government purposes. The Los Alamos National Laboratory requests that the publisher identify this article as work performed under the auspices of the U.S. Department of Energy. Los Alamos National Laboratory strongly supports academic freedom and a researcher's right to publish; therefore, the Laboratory as an institution does not endorse the viewpoint of a publication or guarantee its technical correctness.

Synthetic Seismograms at Regional Distances for May 1995 Earthquake and Explosion Sources in Western China

Fred N. App, Randy J. Bos, James R Kamm
Los Alamos National Laboratory
Project No. ST482A
Sponsored by U. S. Department of Energy

Abstract

Waveforms recorded at several regional seismic stations at varying azimuths from explosion and earthquake sources in Western China exhibit marked variation from station to station. We have performed two-dimensional finite difference simulations of these events, using moment tensor sources and simple crustal structure models, to generate synthetic seismograms at these locations. The synthetic seismograms at three locations exhibit behavior that is qualitatively consistent with the data, while computational results at a fourth station differ from the data. We discuss these results, the assumptions of the simulations, and the limitations of this type of modeling in the context of regional seismic propagation. This report is a condensation of a Los Alamos National Laboratory, LA-UR-96-1600, with the same title.

Keywords:

synthetic seismograms
calculations/simulations
earthquake and explosion sources

Objective

This work is in direct support of U.S. and Comprehensive Test Ban Treaty (CTBT) verification goals. The research is aimed at providing the tools to minimize the frequency of false alerts (conventional explosions, mine collapses, rock bursts, or earthquakes that are mistakenly interpreted to be nuclear tests), yet provide confidence that if there were a nuclear test conducted somewhere in the world it would be recognized as being nuclear. Whereas there are numerous seismograms from earthquakes and other conventional sources for calibrating many areas of the world seismograms from nuclear explosions are relatively rare and from a few very localized regions. One possible way to obtain the nuclear data is through the computer generation of synthetic seismograms using realistic descriptions of the nuclear source and the more important geologic features along the path of the signal.

This is a report on the comparison of such synthetically generated seismograms with measurements in a region around Lop Nor, the Chinese Nuclear Test Site located in Western China using a recently-developed LANL finite-difference code named AFD [1]. The study included calculations for a 15 May 1995 Lop Nor explosion and a 2 May 1995 northwest China earthquake. The objective was to evaluate the code and identify any improvements needed in order to meet requirements.

Research Accomplished

Figure 1 is a graphic with the contour of Moho depth of the region around Lop Nor superimposed on which are surface vertical velocity traces induced by the two seismic sources as recorded at several regional stations. Clockwise from the North these stations are: TLY (ea. 1600 km NE of Lop Nor), ULN (ea. 1600 km ENE), NIL (ea. 1600 km SW), AAK (ea. 1200 km W), and BRVK (ea. 1900 km NW). Depth to Moho is but one of the elements to be taken into account in performing full waveform modeling in such a region. Other potentially important factors are location, depth and lateral extent of sedimentary basins and surface topographic features. As shown in Figure 1, there is notable variation in the recorded broadband waveforms at these various stations. To first order, an explosion is expected to have more of its energy associated with the p-wave (or Pg-the earlier arriving part of the signal) since the source is mostly spherical. Conversely, the earthquake energy should be primarily associated with the s-waves (or Lg-the later arriving signals) since the energy is released through a shearing motion. Upon inspection of the waveforms in Figure 1, it is apparent that such a clear partitioning of energy is true only along certain paths, most notably the path to Station NIL in the lower left-hand corner of the plot. At Stations AAK and BRVK the partitioning is less clear but still in evidence. At Stations TLY and ULN the explosion and earthquake are practically indistinguishable from each other. It is quite apparent that the signal undergoes substantial modification along its path; this observation demonstrates the need for numerous stations and paths for properly characterizing a given signal as being from an explosion or earthquake source. Equally important from the

standpoint of CTBT verification needs, we need to be able to capture these same observed differences in the modeling.

A key feature to be included in the modeling is the crustal structure along each of these paths. The structure information was obtained from the Cornell Middle East / North Africa Project's online Profile maker (which also contains Eurasian data), using Lop Nor as the source location. Specifically, values for the depth-t-basement of sedimentary basins as well as for the Moho depth were obtained along each path. Approximate values for the elastic constants and attenuation factors for each material (sediment, mantle, crust) were assigned. Similarly, the values for the moment tensor coefficients and their time dependence were prescribed. Details on the input parameters used in the calculations are described in Ref. 2; the calculations were run out to simulation times of ca. 500s.

AU calculations were run with the LANL AFD anelastic finite difference code, using moment tensor sources. No detailed source physics, such as strong non-linear motion and surface spallation, was included in these calculations although that is an option in these kinds of calculations. Also, topographic effects were ignored. The simulations were run in a two-dimensional, plane-strain (Cartesian) geometry assuming a flat free surface. It is possible to run the code in either 2-D or 3-D, but the limited capabilities of current compute platforms limit regional-sized calculations to 2-D. Among the implications of these assumptions are: (1) no geometrical dispersion effects are included, (2) 3-D scattering is absent and (3) no surface topography effects are present. The main reason these calculations were run in Cartesian as opposed to cylindrical geometry is that we have not implemented the capability to account for the 3-D moment tensor source into the coding for the cylindrical geometry equations of motion (i.e., the "2-1/2-D" approach). Due to the nature of finite difference simulations, and the memory and speed limitation of the computers available to the research team, the results are limited in frequency content to about one Hz.

Figures 2–5 are graphics containing the crustal sections of each path considered together with the computed surface vertical velocity synthetic seismograms. The crustal structure plots, in which the source location is at the left, have an expanded vertical scale relative to the horizontal scale. For this series of calculations, the same site (Lop Nor) was used for the location of both the earthquake and explosion; in reality, the earthquake was located ca. 400 km WNW of Lop Nor, in a region where there is a small depression in the Moho. In the simulations, the earthquake was centered at a depth of 33 km, and the explosion at 4 km.¹ The vertical scale of the velocities varies between the calculations and experiment so only qualitative comparisons should be made. Additionally, all velocities have been filtered in the passband 0.21-1.0 Hz.

¹This depth of burial (DOB) very likely exceeds the actual DOB associated with this shot. In the simulations, the source must be located several zones beneath the free surface. Therefore, the explosion source was located at a depth of 4 km, corresponding to eight computational zones, in all calculations in this series.

Figure 2 shows the results along the path to AAK, which has a relatively smooth nearly level Moho and virtual absence of sedimentary basins. There is qualitative agreement between the data and simulation for the explosion insofar as the Lg is somewhat enhanced relative to the Pg. Similarly, although somewhat less accurately, the earthquake traces exhibit the canonical “earthquake” property of significantly enhanced Lg relative to Pg. In both simulations there is a strongly attenuated Lg coda (relative to the data), a characteristic that is evident in all simulations shown in this report.

Figure 3 presents the results along the path to NIL, which exhibits a strongly dipping Moho structure along the Tibetan suture zone, as well as a pronounced sedimentary basin. Again, there is approximate qualitative agreement between the data and simulations. The explosion synthetic shows enhanced Pg relative to Lg although not as strongly pronounced as in the data. The earthquake synthetic shows an Lg enhancement relative to Pg that is more pronounced than in the data.

Figure 4 shows the results along the path to TLY, which has a mildly varying Moho and minor sedimentary structure. Approximate qualitative agreement between the data and simulations again obtains. In this case, both explosion and earthquake exhibit the canonical “earthquake” property of much enhanced Lg relative to Pg. In both simulations there is again a strongly attenuated Lg coda.

Figure 5 gives the results along the path to ULN, which differs only slightly in azimuth from the path to TLY (see Fig. 1) and exhibits a similar structure consisting of a mildly varying Moho and negligible sedimentary basin. In this case however, there is notable lack of approximate qualitative agreement between the data and simulations. The waveform data for both explosion and earthquake exhibit an enhanced Pg structure (which is also evident in the broadband data shown in Fig. 1); this feature is not reproduced in the synthetics, which exhibit characteristics similar to those shown in the TLY simulations.

Conclusions and Recommendations

The computational results described above largely exhibit reasonable qualitative agreement with the data. This is a satisfying outcome, insofar as only basic path material, and source information were used as input. Further improvement in this input, using e.g. more refined crustal structure (stratigraphic) models and improved material property information would very likely increase the fidelity of the results to some degree. Similarly, a more refined mesh (i.e., using a smaller computational zone size) would allow for higher frequency resolution in the calculated results.

The computational results, however, also exhibit certain limitations of this method. For example the weak Lg coda in the simulations is likely due to the lack of scattering in the simulations. Presumably this characteristic would be improved by performing 3-D, instead of 2-D, simulations: the enhanced scattering in the 3-D case probably contributes to the Lg

coda. A more serious deficiency is shown in the comparison of the data with computations for the ULN path (see Fig, 5): the calculations do not exhibit at all the Pg structure seen in the data. There are several factors that may plausibly contribute to this discrepancy, among which are (1) the effect of oblique 3-D subsurface structures that cannot be accounted for in the 2-D crustal “slice” simulated, (2) the crustal structure information may be inadequate or incorrect, (3) the material properties used may be inappropriate, (4) near-receiver geology and/or structure effects that were completely absent from the simulation.

Synthetics generated with the current code, even limiting the calculations to 2-D, can provide improved understanding of processes important in shaping waveforms along specific paths. An intrinsic strength of the finite difference technique is that it allows full inspection of the physical processes occurring throughout the entire stress field during the simulations. With proper qualification, the waveforms *may* be useable as crude substitute waveforms in areas for which there is no nuclear explosion data. However, in order to capture all of the salient features of a regional waveform, there is a very real need to install such improvements as topography into the code, optimize the code to minimize memory requirements and execution time, and implement the code onto more powerful compute platforms. As time and resources permit, we intend to develop the capability for using these simulations as an admittedly imperfect substitute for data along paths for which seismic data is either unavailable or unattainable (or both). Given such a capability, the outcome of simulations would be primarily limited by information on the geology.

References

1. J. R. Kamm, R. J. Bos & E. M. Jones *User's Guide to AFD v. 1.0*, Los Alamos National Laboratory report LA-UR-96-853, March, 1996.
2. F. N. App, R. J. Bos & J. R. Kamm, *Synthetic Seismograms at regional Distances for May 1995 Earthquake and Explosion Sources in Western China*, Los Alamos National Laboratory report EA-UR-96-1600.

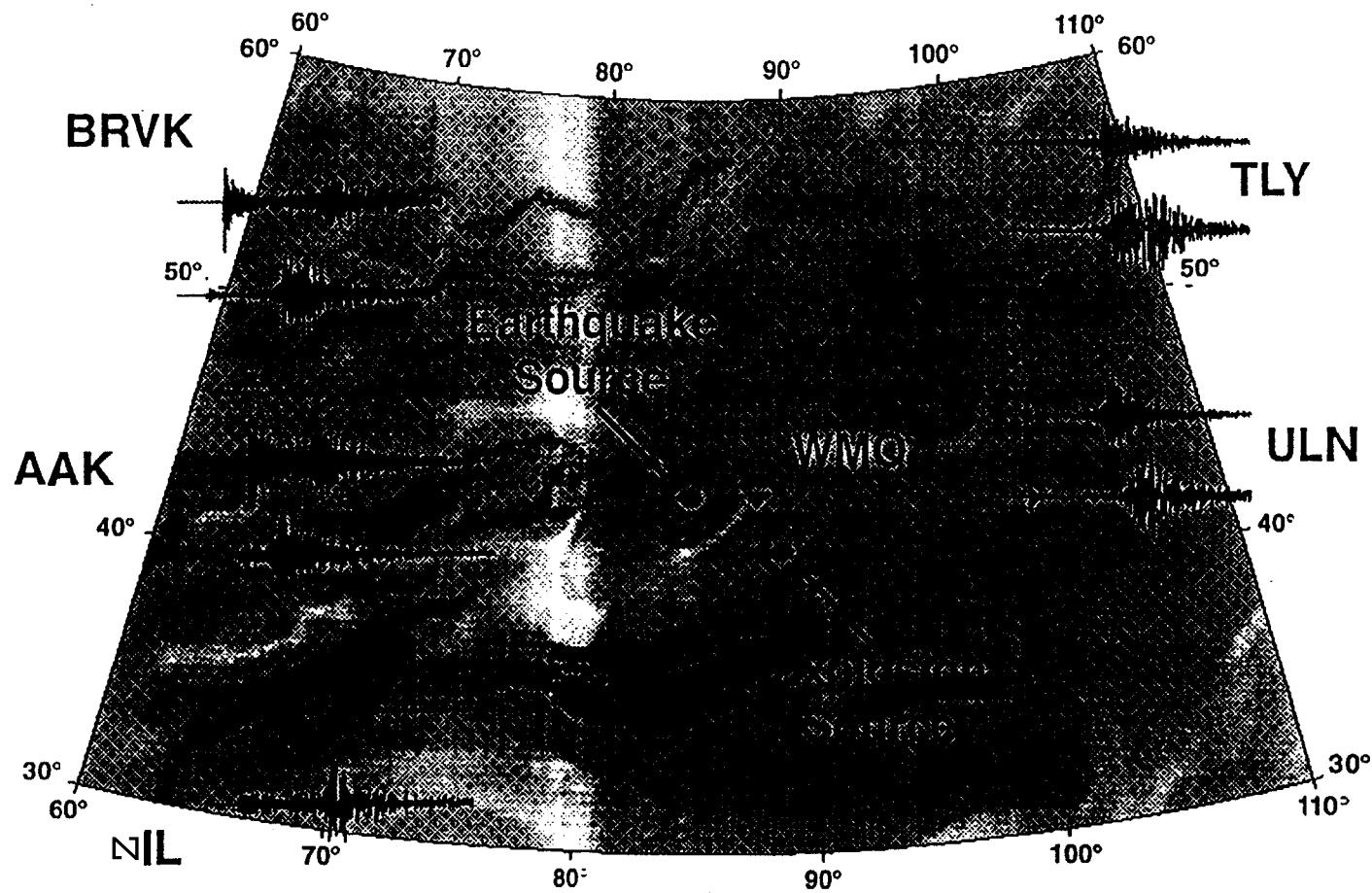


Figure 1. Contour map of Moho depth in Western China, with surface vertical velocity waveforms recorded for the 2 May 1995 magnitude 5.5 earthquake and the 15 May 1995 magnitude 6.1 explosion. The darker regions correspond to greater Moho depth. Inverted triangles denote seismic station locations, with the earthquake waveforms below those of the explosion. There is markedly varying behavior exhibited in the broadband waveforms along the different paths from these sources.

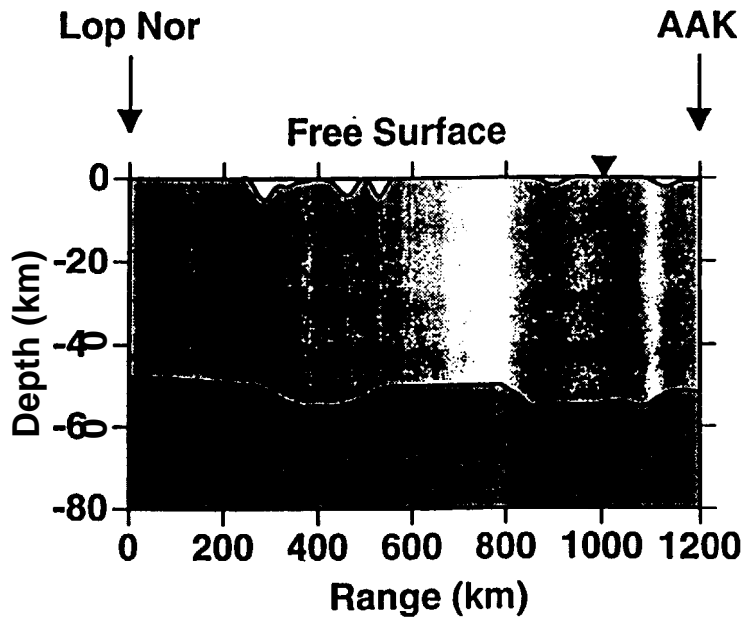
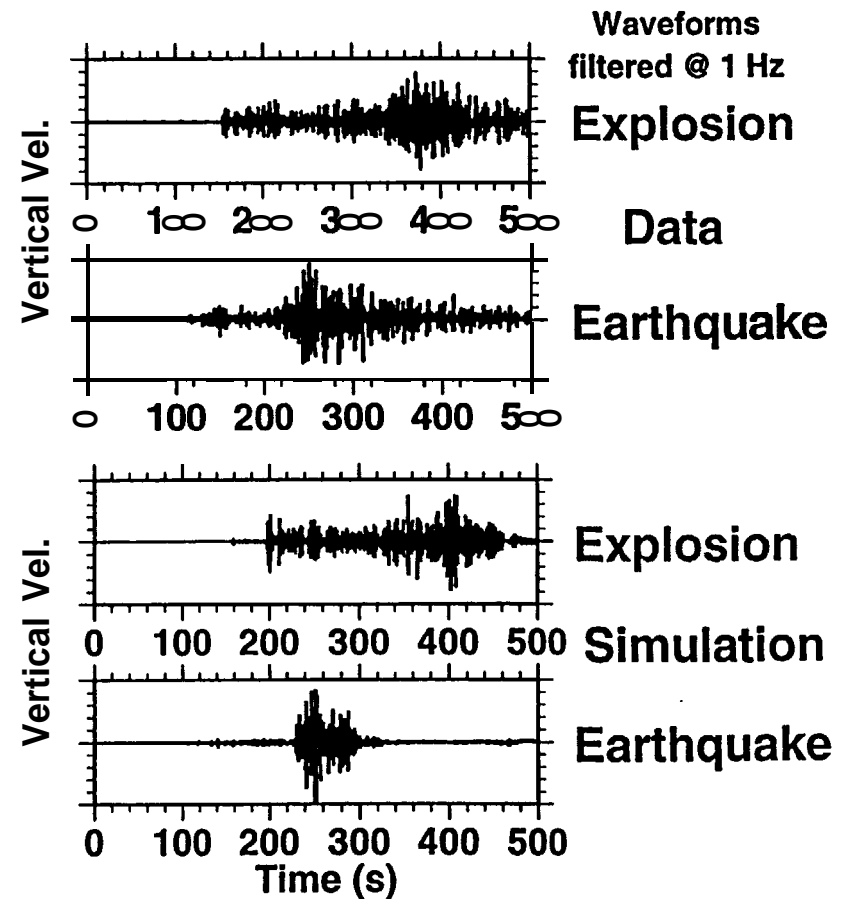


Figure 2. Crustal structure between Lop Nor and station AAK (above), located ca. 1200 km W of Lop Nor; earthquake and explosion waveforms at this station (right). There is approximate qualitative agreement between the data and simulation for both sources. The simulations exhibit a lack of Lg coda, likely due to a lack of scattering in the 2-D calculations.



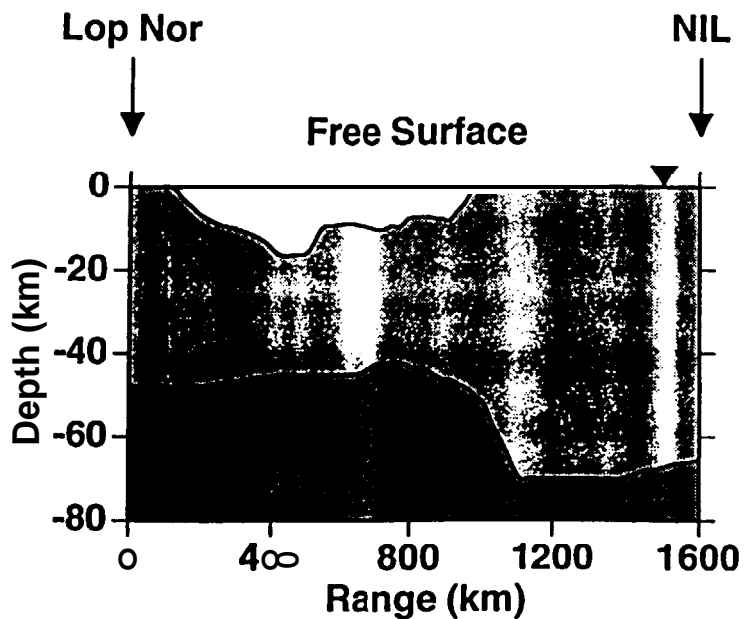
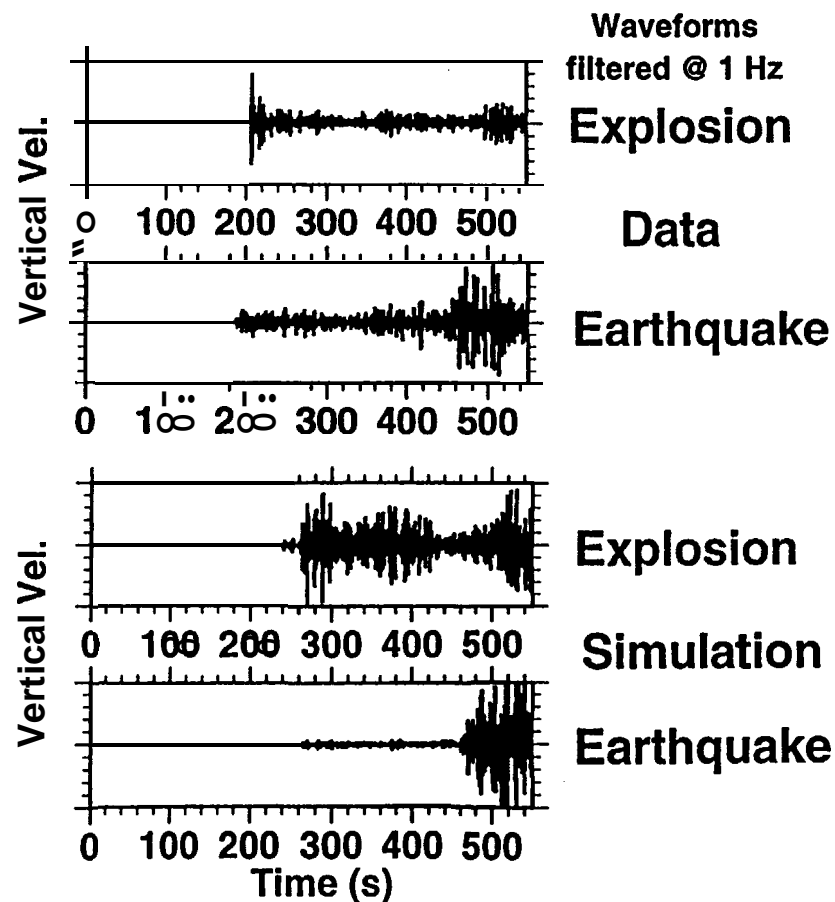


Figure 3. Crustal structure between Lop Nor and station NIL (above), located ca. 1600 km SW of Lop Nor; earthquake and explosion waveforms at this station (right). The path exhibits a strongly dipping Moho as well as a pronounced sedimentary basin. There is approximate qualitative agreement between the data and simulation for both sources.



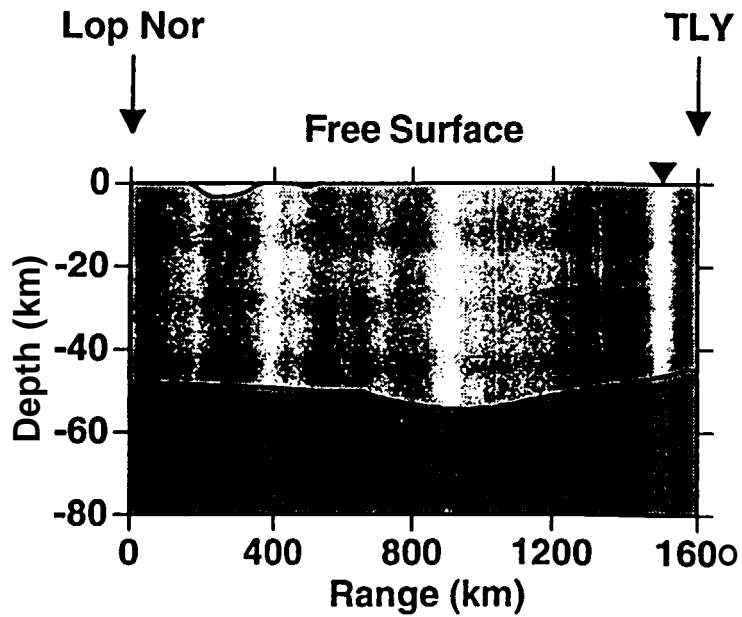
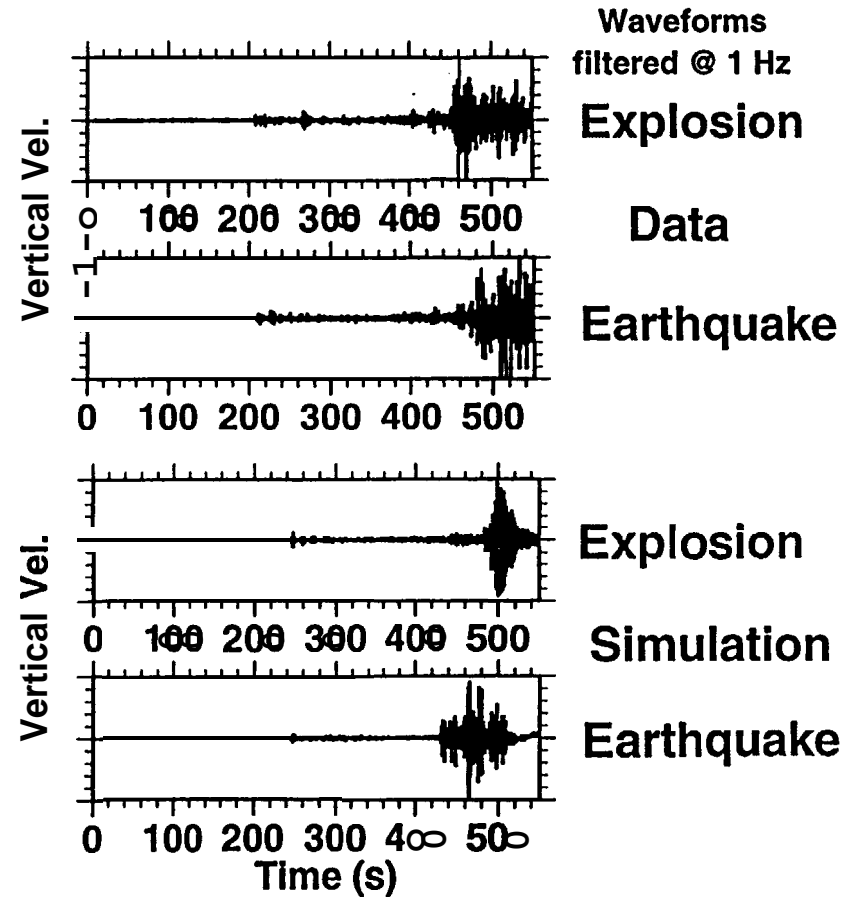


Figure 4. Crustal structure between Lop Nor and station TLY (above), located ca. 1600 km NE of Lop Nor; earthquake and explosion waveforms at this station (right). The path exhibits a mildly varying Moho and minor sedimentary basin. There is approximate qualitative agreement between the data and simulation for both sources, with the exception of the weak Lg coda in the simulations.



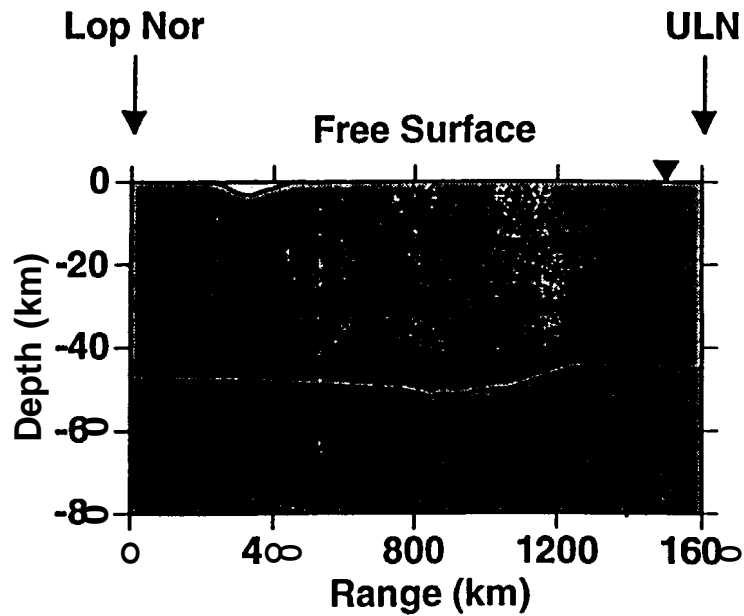


Figure 5. Crustal structure between Lop Nor and station ULN (above), located ca. 1600 km ENE of Lop Nor; earthquake and explosion waveforms at this station (right). The path is similar to that to station TLY (Fig. 4). There is notable disagreement between the data and simulation for these sources: the data for both the earthquake and explosion show a distinctive P_g that is lacking in the corresponding simulations.

